Journal of Molecular Catalysis A: Chemical 353–354 (2012) 87–94

Contents lists available at SciVerse ScienceDirect

Journal of Molecular Catalysis A: Chemical

journal homepage: www.elsevier.com/locate/molcata

Liquid phase photo-deposition in the presence of unmodified β-cyclodextrin: A new approach for the preparation of supported Pd catalysts

S. Scirè[a,*], S. Giuffrida[a,**], C. Crisafulli[a], P.M. Riccobene[a], A. Pistone[b]

[a] Dipartimento Scienze Chimiche, Università di Catania, Viale A. Doria 6, 95125 Catania, Italy
[b] Dipartimento di Chimica Industriale ed Ingegneria dei Materiali, Università di Messina, Contrada di Dio, 98166 Messina, Italy

ARTICLE INFO

Article history:
Received 2 June 2011
Received in revised form 3 November 2011
Accepted 4 November 2011
Available online 15 November 2011

Keywords:
Catalyst preparation
Liquid phase photo-deposition
Nanoparticles
β-Cyclodextrin
Structure sensitive reaction
VOC combustion

ABSTRACT

The preparation of alumina supported Pd catalysts through a photochemical approach, consisting in the liquid phase photo-deposition (LPPD) technique in the presence of unmodified β-cyclodextrin (βCD) as protecting agent, has been here investigated. It was found that it is possible to tune both the Pd nanoparticles size and their distribution over the support surface by changing the concentration of the βCD used during the photodeposition process. In fact, on increasing the amount of the βCD, the obtained Pd/Al_2O_3 samples exhibited Pd nanoparticles (NPs) smaller and more homogeneously distributed over the support, pointing out that the βCD has a protective effect, avoiding the growth of Pd NPs and their aggregation. It is concluded that LPPD in the presence of unmodified β-cyclodextrin represents an interesting approach for the preparation of supported Pd catalysts with a controlled metal nanoparticle size and distribution to be used in structure sensitive reactions.

1. Introduction

The development of metal particles with nanometer size has been intensively pursued because of their technological and scientific relevance [1–3]. These metal nanoparticles (NPs) often exhibit very interesting electrical, optical, magnetic and catalytic properties, which cannot be achieved by their bulk counterparts [4,5]. In particular in the case of applications of NPs for catalytic purposes, the obtainment of nanoparticles with a controlled size is a critical factor chiefly for those reactions which are dependent on particle dimension, the so-called structure sensitive reactions [6]. Recently, we reported the preparation of supported metal (Pt, Pd, Ag) catalysts with a narrow particle size distribution through a photochemical approach, namely the liquid phase photodeposition (LPPD) technique, which allows the direct deposition of active metallic species on the support from the liquid phase at room temperature [7–10]. LPPD involves the chromophore of a metal complex which is able to absorb the light producing a photoexcited state which may decompose, by a photoredox reaction, to give an unprotected solid metallic phase cluster able to spread over the support surface [11,12]. The main advantages of this photochemical approach are the short reaction time, the high reproducibility, the use of a clean reducing agent as the light, the possibility to work at room temperature with simple and low cost equipment.

Ligand or polymers with some affinity for metals have been often used as protecting agents of NPs, preventing them from aggregating through the adsorption of these molecules at the metal particle surfaces, thus providing a protective layer [13]. For instance polyvinylpyrrolidone (PVP) [10,14–16] and cetyltrimethylammoniumbromide (CTAB) [17] have been used for the preparation of supported NPs to be used as heterogeneous catalysts. However, it must be underlined that the presence of residual protecting agent in the final catalyst can be detrimental to catalysis in so as it can constitute a poison, preventing the NPs from activating the reacting molecules or binding to the support [6,16].

In recent years, cyclodextrins (CDs) have been increasingly used in the preparation and the control of metal nanoparticles such as gold [18,19], palladium [20] and platinum [21]. Cyclodextrins are a group of cyclic oligosaccharides composed of several glucopyranose units. The most common CDs are α-, β- and γ-CDs, consisting of six, seven and eight unities respectively [22]. The oligosaccharide forms a truncated cone which allows CDs to form inclusion complexes with small hydrophobic molecules that fit into the cavity. This host–guest interaction may be also applied in drug delivery, chromatography, selective removal of undesired substances and solubility enhancement [21,23].

Among transition metals, Pd is probably one of the most versatile and used in catalysis. It is one of the most efficient metals for the formation of C–C bond [24] in organic reactions such as Suzuki,

* Corresponding author. Tel.: +39 0957385112; fax: +39 095580138.
** Corresponding author.
E-mail addresses: sscire@unict.it (S. Scirè), sgiuffri@unict.it (S. Giuffrida).

1381-1169/$ – see front matter © 2011 Elsevier B.V. All rights reserved.
doi:10.1016/j.molcata.2011.11.009

Table 1
Code and characteristics of investigated Pd catalysts.

Sample code	βCD/Pd(acac)$_2$ molar ratio	Pd content (wt%)	Average Pd diameter (nm)[a]	Pd dispersion (%)[b]	TOF (h^{-1})[c]	T_{50} (°C)[d]
PdAl	0	0.98	10.6	10.4	68	149.1
PdAl-βCD-5	5	0.95	8.8	12.5	164	131.9
PdAl-βCD-30	30	0.92	6.7	16.5	414	126.4
PdAl-βCD-67	67	0.97	5.7	19.4	998	98.5

[a] Estimated by TEM.
[b] Calculated from the average Pd diameter obtained by TEM.
[c] Calculated from conversion values at 110 °C.
[d] Temperature at which 50% methanol conversion was reached.

Heck, Still and Sonogashira couplings [25–27] and for hydrogenation of polyunsaturated hydrocarbons [28,29]. Palladium is known as an efficient electro-catalyst for ethanol oxidation for fuel cell applications [30] and also displays a remarkable performance in H_2 storage and sensing [31,32].

Herein, we report a photochemical approach, consisting in the liquid phase photo-deposition technique in the presence of different amounts of β-cyclodextrin (thereinafter named as βCD), with the aim to prepare γ-alumina supported Pd nanoparticles with a controlled metal size. We like to stress the fact that we used an unmodified βCD, i.e. a βCD without any functional group, in order to allow its easy removal from the catalyst surface by washing with the solvent used in the preparation. To our knowledge, this is the first attempt to use unmodified βCD to control the size of supported palladium nanoparticles to be used as heterogeneous catalysts. Catalytic activity of prepared catalysts was evaluated in the deep oxidation of methanol, which was chosen as representative of volatile organic compounds (VOC).

2. Experimental

The bis(2,4-pentandionato) Pd(II) complex, Pd(acac)$_2$, and β-cyclodextrin (Aldrich) were reagent grade. Ethanol (Carlo Erba), was spectrophotometric grade. γ-Al_2O_3 used as support was from Alfa Aesar with a grain size of 106–180 μm and a BET surface area of 216 $m^2\,g^{-1}$.

The kinetics of Pd(acac)$_2$ photodegradation in the absence of the support were followed spectrophotometrically in a quartz cuvette (3 mL) with a Jasco V-560 spectrophotometer using a light intensity of 1.0×10^{-5} Nhν min^{-1}. It must be noted that a linear correlation between absorbance and concentration was obtained both for Pd(acac)$_2$ and Hacac solutions, pointing out that, in the concentration range of this work, no interaction occurs among the molecules of each species.

For the preparation of alumina supported Pd catalysts by LPPD, the suitable amount of Pd(acac)$_2$ (9.15 mg) was dissolved in 50 mL of ethanol in a quartz vessel, then water was added until 200 mL obtaining a water/ethanol (75/25, v/v) solution, where a little amount of Pd(acac)$_2$ remained unsolved. Successively three different amounts of βCD were added so to obtain fully clear solutions with concentrations of 1.0×10^{-2} M, 4.5×10^{-3} M and 7.5×10^{-4} M. The support (γ-Al_2O_3, 310 mg) was then suspended in the solution under continuous stirring. The irradiation was then performed, at 25 °C, in nitrogen atmosphere, using a Rayonet Photochemical Reactor equipped with various numbers of lamps, provided by Italquartz, with monochromatic emission at 254 nm. The light intensity, measured by a ferric oxalate actinometer [33], was 1.0×10^{-5} Nhν min^{-1} (27 mW cm^{-2}). The vessel suspension was subjected, during the irradiation, to fast and continuous stirring to avoid the sedimentation of the γ-Al_2O_3. The advancement of the photoreduction was followed spectrophotometrically taking, at various times without stopping the irradiation, a little aliquot of the solution which was centrifuged before the spectrophotometric analysis. The complete disappearance of the absorption peak at 324 nm (at this wavelength the released ligand Hacac does not absorb) indicated the end of the reaction. After completion of the photochemical deposition of the metal onto γ-Al_2O_3, the suspended material was recovered by centrifugation and washed several times with water and ethanol and then dried in an oven at 90 °C. All Pd samples were prepared in order to have a nominal 1 wt.% Pd content. Real Pd loadings, determined by atomic adsorption spectrometry, are reported in Table 1.

FTIR spectra were recorded in the frequency range of 4000–700 cm^{-1} on a Perkin-Elmer System 2000 spectrophotometer equipped with a triglycine sulfate (TGS) detector, with 2 cm^{-1} resolution.

High resolution transmission electron microscopy was carried out on a 200 KeV JEOL JEM 2010 analytic electron microscope (LaB6 electron gun), equipped with a Gatan 794 Multi-Scan CCD camera for digital imaging. A drop of the clear Pd–βCD solution (samples in the absence of the support, the so-called naked samples) or of the Pd–βCD-alumina suspension (supported samples prepared by 2 min ultrasonic treatment in isopropyl alcohol) was placed onto a carbon-coated copper micro-grid followed by evaporating off the solvent under ambient conditions. In order to obtain a good statistical particle size distribution several different areas of the grid were observed and more than 150 Pd particles measured for each sample. The average size diameter estimated by TEM was calculated using the following formula: $d = \Sigma(n_i d_i)/n$, where n_i is the number of Pd particles of diameter d_i and n is the total number of Pd particles. Pd dispersion values (reported in Table 1) were calculated by the average Pd size obtained by TEM. Before TEM analysis supported Pd samples were treated in H_2 at 150 °C for 1 h and then calcined in air at 200 °C for 1 h.

Catalytic activity tests were performed in a continuous-flow fixed-bed microreactor in the gas phase at atmospheric pressure, using 0.05 g of catalyst (80–140 mesh) diluted with an inert glass powder. The reactant mixture was fed to the reactor by flowing a part of the He stream through a saturator containing the VOC and then mixing with O_2 and He before reaching the catalyst. The reactant mixture was 0.7 vol.% methanol and 10 vol.% O_2, balance in helium. A space velocity (GHSV) of 7.6×10^{-3} mol h^{-1} $g^{-1}{}_{cat}$ was always used. The effluent gases were analysed on-line by a gas chromatograph (Thermo), equipped with a packed column with 10% FFAP on Chromosorb W and FID detector, and by a quadrupole mass spectrometer (VG quadrupoles). For all experiments CO_2 was the main carbon-containing product, only very small amounts of CO were found at low conversions. The carbon balance was always higher than 95%. Before activity tests samples were treated in H_2 at 150 °C for 1 h and then calcined in air at 200 °C for 1 h. Preliminary runs carried out at different flow-rates showed the absence of external diffusional limitations. The absence of internal diffusion limitations was verified by running experiments with catalyst powders at different grain size.

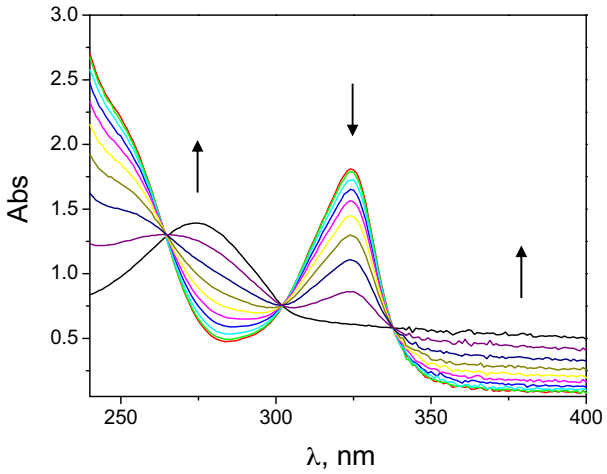

Fig. 1. Spectral changes of a water/ethanol solution (75/25, v/v) of $Pd(acac)_2$ 1.5×10^{-4} M and βCD 1.0×10^{-2} M irradiated at 254 nm ($I = 1.0 \times 10^{-5}$ Nhν min^{-1}) at various times 0–18′. The spectra were registered every 2 min.

Code and characteristics of Pd samples are summarized in Table 1.

3. Results

3.1. Kinetic of the Pd complex photoreduction and preparation of alumina supported Pd catalysts

$Pd(acac)_2$ is completely insoluble in water but it is fairly soluble when the βCD is present in the aqueous solution, due to the complete or partial inclusion of the $Pd(acac)_2$ complex within the cyclodextrin cavity. Nevertheless the maximum $Pd(acac)_2$ solubility at the highest possible βCD concentration in aqueous solution (1.0×10^{-2} M) was lower than that required to prepare a sufficient amount of catalyst. Therefore we used a water/ethanol (75/25, v/v) mixture to solve both the $Pd(acac)_2$ and the βCD. Under these latter conditions a part of $Pd(acac)_2$ likely forms an inclusion complex with the cyclodextrin, the remaining part is instead free, i.e. not interacting with the βCD. The relative amount of these two species reasonably depends on the βCD concentration, according to the following equilibrium:

$$Pd(acac)_2 + \beta CD \rightleftharpoons Pd(acac)_2$$

-βCD, as also confirmed by kinetic data reported hereinafter.

In Fig. 1 the spectral changes caused by irradiation at 254 nm of the water/ethanol (75/25, v/v) solution of $Pd(acac)_2$ 1.5×10^{-4} M and βCD 1.0×10^{-2} M are reported as a representative example for the three βCD concentrations used in this work. It must be underlined that in the photoreduction process the incident light (254 nm) is absorbed essentially from the $Pd(acac)_2$ complex, whereas the absorption from the βCD is negligible. Figure shows that spectral changes consisted in the decrease of the absorption band at 324 (ε = 12,000) nm, the appearance of a new band at 274 nm, typical of Hacac (λ_{max} = 274 nm, ε = 3000), consistent with a π–π^* (HOMO–LUMO) transition [34], and of a moderate structureless absorbance over 350 nm, attributed to the light scattering of Pd colloidal nanoparticles. It must be noted that Pd nanoparticles do not exhibit the UV–vis plasmon band due to the damping effect of *d*–*d* transitions [35]. As the reaction proceeded, the solution colour turned from pale yellow to brown. At the end of the photoreduction, the released ligand concentration, detected by UV spectrophotometer, was the double of the amount of the starting complex concentration. It must be underlined that the $Pd^{II}(acac)_2$ complex is unreactive upon irradiation at wavelength >260 nm, due to the presence of low-energy metal-localized *d*, *d* singlet state [36]. Interestingly, when the concentration of the βCD decreased the time required to complete the photoreduction process increased, moving from 18′ (βCD concentration of 1.0×10^{-2} M) to 55′ (βCD concentration of 4.5×10^{-3} M), up to 100′ in the experience carried out without the βCD (in pure ethanol). The kinetics of the photoreduction process for the above samples, expressed as $Pd(acac)_2$ conversion versus irradiation time, were reported as supplementary information. It must be reminded that in all experiments the $Pd(acac)_2$ concentration was always kept constant.

According to these findings we propose a photoreduction mechanism, analogous to that previously reported [10,37], which involves two sequential Pd–O homolytic cleavages, the first of $Pd^{II}(acac)_2$ and the second of $Pd^{I}(acac)$ formed in the previous step, with formation of two acetylacetonyl radicals that can abstract hydrogen atoms both from βCD and ethanol, depending on their relative concentrations. The route of the H-abstraction from βCD (intra-cage or bimolecular acac•-βCD collision) is expected to be highly efficient because of the presence of 14 available hydrogen atoms bonded to secondary carbons and close to the radical center [38,39], whereas the H-abstraction from ethanol is more difficult. It must be also noted that hydrogen abstraction from water molecules is not allowed because thermodynamically not favoured [21]. Therefore the kinetic indicates that the ease of H-abstraction of acac• from different targets is in the order: intra-cage βCD > bimolecular acac•-βCD collision > bimolecular acac•-ethanol collision.

For the preparation of supported Pd catalysts the photoreduction was carried out in the presence of alumina as support under the same conditions of kinetic experiments. In this case the spectral changes were the same as those observed in the absence of the support, but the photoreduction required a longer irradiation time in order to reach the completion. For instance when the photoreduction was carried out with a solution of 1.5×10^{-4} M $Pd(acac)_2$ and 1.0×10^{-2} M βCD without the support, 18′ were necessary to complete the reaction, whereas in the presence of the support 1 h ca. of irradiation was required. According to the literature this can be reasonably explained considering that solid alumina particles may partially scatter the incident light [9].

In order to verify if residual βCD was still present on prepared Pd/Al_2O_3 catalysts, we carried out FTIR analyses of washed and unwashed samples and for comparison of pure βCD and alumina (Fig. 2). The IR spectrum of the pure βCD (Fig. 2, curve a) shows a broad band with an absorption maximum centered at about 3340 cm^{-1}, due to the O–H stretching vibrations of the different hydroxyl groups of the βCD [40,41]. A band at 1647 cm^{-1}, related to the bending vibrations of these OH groups, is also well visible. The spectrum presents several other bands, mainly at 2926 cm^{-1} (C–H stretching vibrations of the CH and CH_2 groups), at 1411, 1368, 1335, 1301, 1246 cm^{-1} due to C–H bending vibrations, and at 1154, 1080 and 1027 cm^{-1} attributed to the C–O stretching vibrations of the bonds in the ether and hydroxyl groups. Finally typical bands in the region 1000–700 cm^{-1}, belonging to the rocking vibrations of the C–H bonds and the C–C skeletal vibrations in the glucopyranose ring, are also present [40,41]. The main features of the spectrum of the pure support (Fig. 2, curve d) are bands at 3400 cm^{-1} (O–H stretching), 1646 cm^{-1} (O–H bending) and 850 cm^{-1} (Al–O stretching). The FTIR spectrum of the alumina supported Pd sample prepared in the presence of the βCD at the highest concentration (PdAl-βCD-67 sample) and obtained by centrifugation without any washing exhibits (Fig. 2, curve b) the characteristic bands of the alumina together with some features of very small intensity (bands at 2926, 1647, 1411, 1154, 1080, 1027 cm^{-1}) due to the presence of residual βCD, thus pointing that the most part of the βCD remains in the supernatant solution

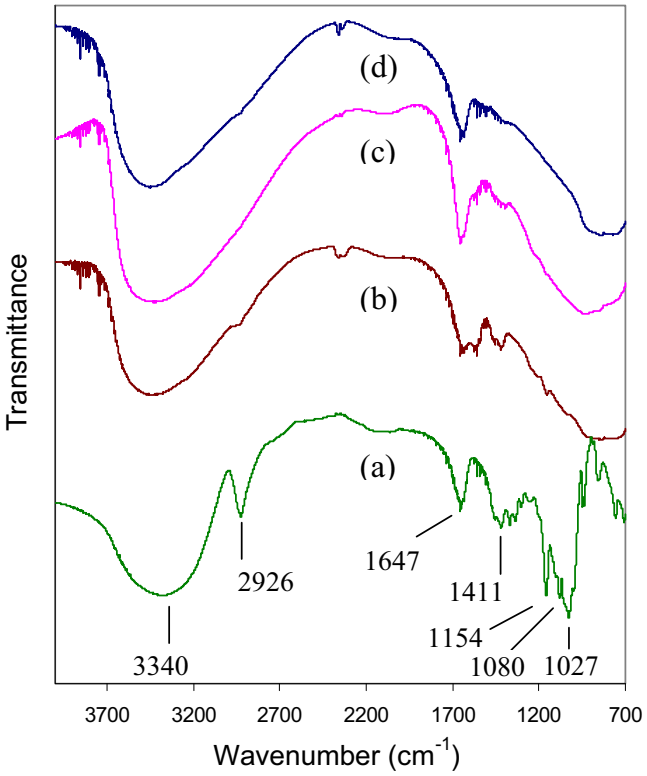

Fig. 2. FTIR spectra of investigated samples: (a) pure βCD; (b) unwashed PdAl-βCD-67; (c) washed PdAl-βCD-67; (d) pure alumina.

during the centrifugation. The washing procedure adopted appears to be highly effective in the removal of almost all the protecting agent, as well evidenced by the FTIR spectrum of the washed sample (Fig. 2, curve c), which is almost the same of the pure alumina one. It is also noteworthy that the IR bands of the βCD in the presence or absence of the Pd particles are substantially at the same wavenumbers providing no evidence of Pd–βCD interaction.

3.2. TEM analysis of naked Pd particles and alumina supported Pd catalysts

In order to characterize metallic palladium nanoparticles, transmission electron microscopy was carried out both on unsupported Pd particles (thereinafter called naked samples) and alumina supported Pd samples. The results are reported respectively in Figs. 3 and 4. Analysis of the spacing of the lattice fringes of 0.224 nm and 0.12 nm for the (1 1 1) lattice planes of palladium and alumina nanoparticles respectively, provided unambiguous discrimination of the two phases.

TEM microphotographs of the samples prepared by carrying out the photoreduction in the absence of the support (naked samples) are reported in Fig. 3. The figure shows that the naked sample with the lowest βCD concentration (Fig. 3a) exhibits large aggregates (>50 nm) constituted by many Pd nanoparticles. When the βCD concentration increases the size of these aggregates decreases to about 40–50 nm on the sample with intermediate βCD concentration (Fig. 3b) down to 10–20 nm on the sample with the highest βCD concentration (Fig. 3c). These results point out that the β-cyclodextrin plays a significant role in preventing the agglomeration of Pd nanoparticles, the higher the βCD concentration the more effective this segregation effect.

Fig. 4 reports TEM photos and size distribution diagrams of alumina supported Pd samples prepared both in the absence of βCD and in the presence of three different βCD concentrations.

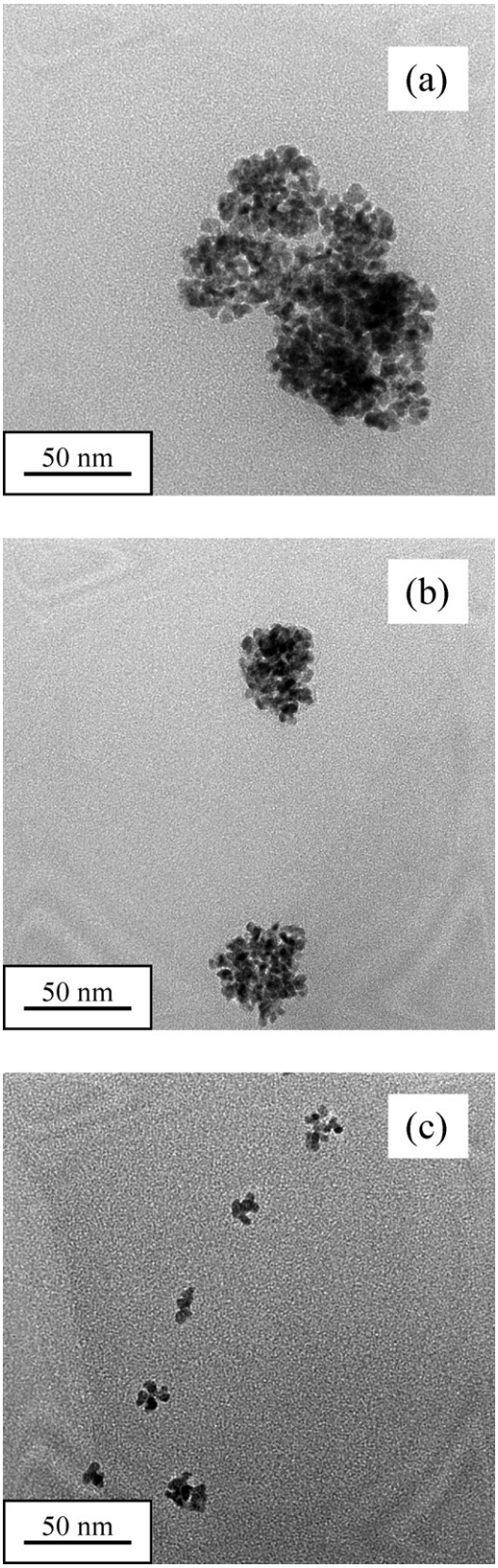

Fig. 3. TEM photographs of naked Pd samples: (a) Pd-βCD-5; (b) Pd-βCD-30; (c) Pd-βCD-67.

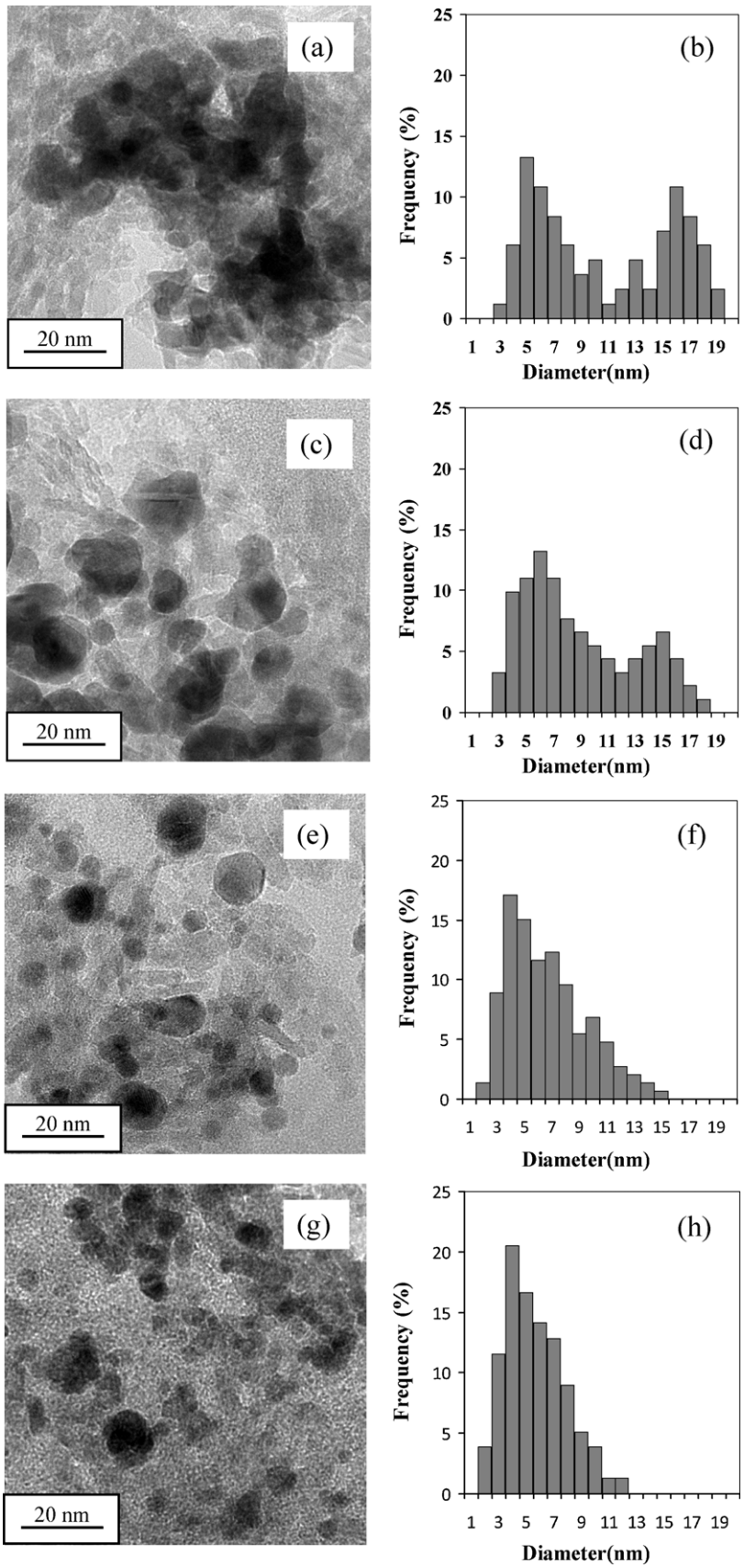

Fig. 4. TEM photographs (a, c, e, g) and Pd distribution (b, d, f, h) of alumina supported Pd samples: (a and b) PdAl; (c and d) PdAl-βCD-5; (e and f) PdAl-βCD-30; (g and h) PdAl-βCD-67.

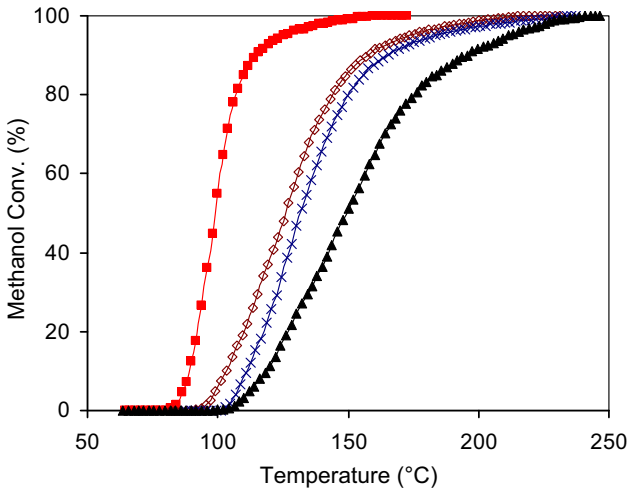

Fig. 5. Conversion of methanol versus reaction temperature over alumina supported Pd catalysts: (▲) PdAl; (X) PdAl-βCD-5; (◇) PdAl-βCD-30; (■) PdAl-βCD-67.

On all Pd/Al_2O_3 samples the TEM images (Fig. 4a, c, e and g) show the presence of almost spherical Pd particles. On the sample prepared without βCD (PdAl) the Pd particles (Fig. 4a) appear to be not well homogeneously spread over the support surface with evident formation of Pd aggregates composed by several distinct Pd particles. These Pd particles range from 3 to 19 nm (Fig. 4b), showing a bimodal distribution having two maxima of comparable height, centered at 5 and 16 nm, with an overall average diameter of 10.6 nm. The TEM photo (Fig. 4c) and the relative size distribution (Fig. 4d) of the sample prepared in the presence of the βCD at the lowest concentration (PdAl-βCD-5) show, analogously to that found on the PdAl sample, Pd particles with diameters ranging from 3 to 18 nm, with a bimodal distribution with two maxima (6 nm and 15 nm). However it can be noted that in this case the second maximum (15 nm) is sensibly less intense than the first one (6 nm), with a resulting average size diameter of 8.8 nm, lower than that found on the sample prepared without βCD. Moreover the Pd nanoparticles appear to have a lower aggregation degree compared to PdAl sample. In the case of the sample with an intermediate βCD concentration (PdAl-βCD-30), Pd nanoparticles are clearly more separate and therefore better distributed over the support (Fig. 4e). Size distribution data (Fig. 4f) show Pd particles from 3 to 15 nm with a rather broad monomodal distribution, centered at 4–5 nm and with an evident shoulder at higher values. The average diameter estimated by this distribution was 6.7 nm. Finally on the sample with the highest βCD concentration (PdAl-βCD-67), TEM data point to a more symmetrical and narrower size distribution of Pd nanoparticles, ranging from 2 to 11 with an average diameter of 5.7 nm (Fig. 4g and h). Analogously to the previous sample, the Pd nanoparticles appear to be well separated from each other and homogeneously distributed over the support. It is interesting to note that the smallest Pd particles obtained in this work (average diameter of 5.7 nm) were anyway bigger than Pt ones (diameters in the range of 1.6–2 nm) achieved through the same LPPD approach and on the same support, even in the absence of any protective agent [7], pointing out that, under our preparation conditions, Pt has a lower tendency to aggregate compared to Pd.

3.3. Catalytic activity

The conversion of methanol as a function of the reaction temperature over investigated Pd/Al_2O_3 catalysts is reported in Fig. 5. It must be noted that on these catalysts, analogously to that reported in the case of Pt/Al_2O_3 [7], the oxidation reaction proceeds directly to CO_2 with no significant formation of intermediate oxidation products (formaldehyde or formic acid). It must be also underlined that on the pure alumina support no reaction was observed up to 250 °C. Fig. 5 shows that on the Pd sample prepared in the absence of βCD (PdAl sample) the reaction starts at around 100 °C, reaching 50% and 100% conversion values at 150 °C and 230 °C ca. respectively. On Pd samples prepared in the presence of βCD the oxidation activity was sensibly higher, increasing on increasing the βCD concentration. Interestingly on the most active sample (PdAl-βCD-67) the reaction starts at around 80 °C and reaches 50% and 100% conversion values at 100 °C and 150 °C respectively, i.e. 50 °C and 80 °C less than on the sample prepared without the protecting agent. In order to allow an easier comparison among various samples, the extrapolated temperatures at which the 50% conversion were reached (T_{50}), together with turnover frequecies (TOF), namely the specific activity per surface Pd atom calculated from conversion values at 110 °C, are summarized in Table 1. It can be noted that, on increasing the βCD concentration used during the photoreduction process, T_{50} values decrease whereas TOFs undergo a significant increase.

4. Discussion

Kinetic data of the photoreduction process, reported in Section 3, showed that irradiation at 254 nm of the Pd complex in ethanol/water and different amounts of βCD, both in the absence and in the presence of the support (alumina), caused the complete photoreduction of Pd(II) to Pd°, which spread over the support. It was found that the presence of the βCD increased the rate of the photoreduction process, according to the proposed mechanism, which involves the Pd–O homolytic cleavage of the starting $Pd^{II}(acac)_2$ complex and of the intermediate $Pd^{I}(acac)$ with final formation of Pd° and two acac radicals that can abstract hydrogen atoms both from the βCD and the ethanol, depending on their relative concentrations.

TEM analysis of the Pd/Al_2O_3 catalysts prepared by LPPD showed that the presence of the βCD during the photoreduction process significantly affects the size of the obtained Pd particles and their distribution over the support, with an effect strongly dependent on the βCD concentration. In particular it was found that the sample prepared in the absence of the βCD exhibits Pd particles heterogeneously distributed over the support surface, forming aggregates composed by several distinct Pd particles having diameters from 3 to 19 nm. The size distribution of these Pd particles was bimodal with two maxima (5 and 16 nm of diameter) of comparable height, with an overall average diameter of 10.6 nm. In the presence of the βCD at the lowest concentration the Pd particles showed always a bimodal distribution, but with the second maximum (at 15 nm) sensibly less intense than the other one (6 nm), resulting in a smaller average particle diameter (8.8 nm). Moreover on this latter sample the Pd nanoparticles had a lower aggregation degree compared to the sample prepared without βCD. On increasing the βCD concentration the Pd particles became smaller, with a monomodal and narrower size distribution and a lower aggregation extent. These results point out that the βCD plays an important role during the preparation of supported Pd catalysts avoiding the growth and the further aggregation of Pd particles on the support surface. This protective effect of the βCD was also verified in the photoreduction of $Pd(acac)_2$ in the absence of the support. In fact TEM of naked samples showed that on increasing the $\beta CD/Pd(acac)_2$ ratio the size of Pd aggregates decreased from more than 50 nm on the sample with the lowest βCD concentration down to 10–20 nm on the sample with the highest βCD concentration.

In order to rationalize the above results we propose that the peculiar microenvironment of the βCD macrocycle can be involved

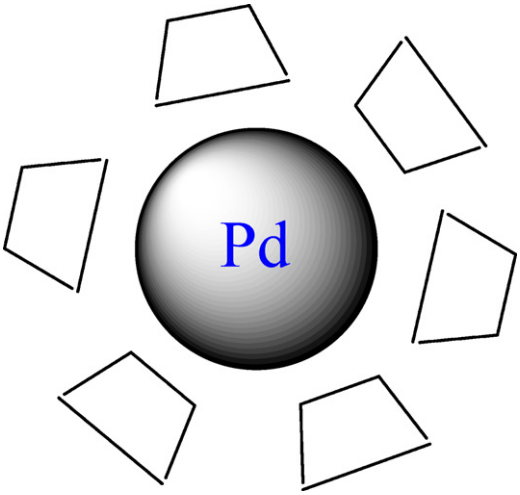

Fig. 6. Schematic representation of the Pd–βCD interaction.

in the formation and size control of Pd nanoparticles, during the LPPD process, in three different ways. Firstly, the non-polar βCD cavity contributes, together with ethanol, to the solubilisation of the photoactive component ($Pd(acac)_2$ complex), otherwise not fully soluble in the water/ethanol mixture. It should be noted that solubilisation of hydrophobic molecules by CDs does not necessarily imply molecular sizes compatible with those of the cavity. For example, it is well-known that very large aromatic hydrocarbons become soluble in the presence of CDs because of effective hydrophobic interactions involving the cavity and part of such hydrocarbons [42,43]. A second action of the βCD derives from the ability of its cage to trap the photogenerated reactive acac radical, enhancing the rate of the Hacac formation, thus resulting in a quicker photoreduction. This increase in the kinetic of the photoreduction process could justify the formation of smaller Pd nanoparticles observed in the presence of growing concentrations of βCD in the LPPD process. In fact it is recognized that the metal cluster dimension depends on the ratio of the nucleation rate to the growing rate of metal particles, an higher ratio leading to smaller particles [9,10,44,45]. A third important role of the βCD is its protective effect against the aggregation of Pd nanoparticles. According to the literature [19,21,46] it seems likely that this effect can be due to hydrophobic interactions between the Pd nanoparticle and several βCD molecules surrounding it (see Fig. 6). In fact, since the internal diameter of the βCD cavity is 0.78 nm and the average dimension of the Pd nanoparticles is much larger (5.7 on the sample with the smallest average sizes) it can be ruled out that the protective effect of βCD is a result of the inclusion of Pd atoms in the CD cavity.

Concerning with the catalytic performance of the Pd/Al_2O_3 samples prepared by LPPD it was found that the samples prepared in the presence of βCD exhibited a higher methanol deep oxidation activity, which increased on increasing the βCD concentration. In order to rationalize these findings it is important to recall that over platinum and palladium catalysts supported on non reducible oxides (such as alumina) the deep oxidation of light alkanes, aromatic hydrocarbons and oxygenated compounds is regarded as a structure sensitive reaction, involving the activation of the oxygen on the noble metal [47]. However conflicting results were reported in the literature on the extent of this size effect as well as on which metal particle size is the optimal one, depending on several factors, such as the metal, the support and the VOC considered [7–10,47–53]. Catalytic results reported in the present paper confirm that the methanol combustion on Pd/Al_2O_3 is a structure sensitive reaction, pointing out that, at least under our experimental conditions and in the considered range of Pd particle size, the catalytic activity increases as the average Pd particle size decreases, as also confirmed by turnover frequencies (TOF), namely the specific activity per surface Pd atom, which are reported in Table 1. Interestingly TOF data show that the increase in the activity becomes more evident when the average Pd particle diameter approaches 5 nm (sample prepared with the highest βCD concentration). This is in good agreement with our previous results, which showed that, on Pd/Al_2O_3 catalysts, Pd particles in the range of 4–5 nm provide a highly efficacious oxygen activation [10]. The occurrence of an optimal Pd metal size for oxygen activation has been also recently demonstrated on Pd/TiO_2 catalysts [54].

5. Conclusions

On the basis of the results reported in the present paper it can be concluded that the LPPD approach carried out in the presence of unmodified βCD as protecting agent represents a reliable method for the preparation of alumina supported Pd catalysts to be used in structure sensitive reactions, such as the VOC combustion. This technique allows, in fact, to tune the Pd nanoparticles size and their distribution over the support surface by changing the concentration of the βCD. A further advantage of this approach was the ease and complete removal of the βCD from the catalytic surface by simple washing, thus avoiding that the presence of residual ligand can be detrimental to catalysis.

Appendix A. Supplementary data

Supplementary data associated with this article can be found, in the online version, at doi:10.1016/j.molcata.2011.11.009.

References

[1] A.P. Alivisatos, Science 271 (1996) 933–937.
[2] H. Weller, Angew. Chem. Int. Ed. 32 (1993) 41–53.
[3] K.J. Klabunde, Nanoscale Materials in Chemistry, Wiley-Interscience, New York, 2001.
[4] A. Doyle, S.K. Shaikhutdinov, S.D. Jackson, H.J. Freund, Angew. Chem. Int. Ed. 42 (2003) 5240–5243.
[5] R.J. White, R. Luque, V. Budarin, J.H. Clark, D.J. Macquarrie, Chem. Soc. Rev. 38 (2009) 481–494.
[6] B.C. Gates, Catalytic Chemistry, John Wiley and Sons, New York, 1992.
[7] C. Crisafulli, S. Scirè, S. Giuffrida, G. Ventimiglia, R. Lo Nigro, Appl. Catal. A: Gen. 306 (2006) 51–57.
[8] S. Scirè, C. Crisafulli, S. Giuffrida, C. Mazza, P.M. Riccobene, A. Pistone, G. Ventimiglia, C. Bongiorno, C. Spinella, Appl. Catal. A: Gen. 367 (2009) 138–145.
[9] S. Scirè, C. Crisafulli, S. Giuffrida, G. Ventimiglia, C. Bongiorno, C. Spinella, J. Mol. Catal. A: Chem. 333 (2010) 100–108.
[10] S. Scirè, S. Giuffrida, C. Crisafulli, P.M. Riccobene, A. Pistone, J. Nanopart. Res. 13 (2011) 3217–3228.
[11] A. Peled, Lasers Eng. 6 (1997) 41–79.
[12] S. Giuffrida, L.L. Costanzo, G.G. Condorelli, G. Ventimiglia, I.L. Fragala', Inorg. Chim. Acta 358 (2005) 1873–1881.
[13] H. Hirai, N. Toshima, in: Y. Iwasawa (Ed.), Tailored Metal Catalysts, D. Reidel, Dordrecht, 1986, pp. 87–140.
[14] T. Taranishi, M. Miyake, Chem. Mater. 10 (1998) 594–600.
[15] J.M. Nadgeri, M.M. Telkar, C.V. Rode, Catal. Commun. 9 (2008) 441–446.
[16] H. Einaga, M. Harada, Langmuir 21 (2005) 2578–2584.
[17] L. Piccolo, A. Valcarcel, M. Bausach, C. Thomazeau, D. Uzio, G. Berhauet, Phys. Chem. Chem. Phys. 10 (2008) 5504–5506.
[18] J. Liu, S. Mendoza, E. Roman, M.J. Lynn, R. Xu, A.E. Kaifer, J. Am. Chem. Soc. 121 (1999) 4304–4305.
[19] Y. Liu, K.B. Male, P. Bouvrette, J.H.T. Luong, Chem. Mater. 15 (2003) 4172–4180.
[20] J. Alvarez, J. Liu, E. Roman, A.E. Kaifer, Chem. Commun. (Cambridge, UK) (2000) 1151–1152.
[21] S. Giuffrida, G. Ventimiglia, S. Petralia, S. Conoci, S. Sortino, Inorg. Chem. 45 (2006) 508–510.
[22] J. Szejtli, in: J.L. Atwood, J.E.D. Davies, D.D. Macnicol, F. Vogtle (Eds.), Comprehensive Supramolecular Chemistry, vol. 3, Pergamon-Elsevier, New York, 1996, pp. 5–40.
[23] D. Bonacchi, A. Caneschi, D. Gatteschi, C. Sangregorio, R. Sessoli, A. Falqui, J. Phys. Chem. Solids 65 (2004) 719–722.
[24] D. Astruc, Inorg. Chem. 46 (2007) 1884–1894.
[25] R. Franzèn, Can. J. Chem. 78 (2000) 957–962.
[26] S.W. Kim, W.Y. Lee, T. Hyeon, J. Am. Chem. Soc. 124 (2002) 7642–7643.

[27] S.U. Son, Y. Jang, J. Park, H.B. Na, H.M. Park, H.J. Yun, J. Lee, T. Hyeon, J. Am. Chem. Soc. 126 (2004) 5026–5027.
[28] T. Ouchaib, J. Massardier, A. Renouprez, J. Catal. 119 (1989) 517–523.
[29] T. Redjala, H. Remita, G. Apostulescu, M. Mostafavi, C. Thomazeau, D. Uzio, Gas Oil: Sci. Technol. 61 (2006) 789–797.
[30] S.S. Gupta, J. Datta, J. Power Sources 145 (2005) 124–132.
[31] F. Favier, E.C. Walter, M.P. Zach, T. Benter, R.M. Penner, Science 293 (2001) 2227–2231.
[32] C. Langhammer, I. Zoric, B. Kasemo, Nano Lett. 7 (2007) 3122–3127.
[33] J. Calvert, J.N. Pitts, Experimental Methods in Photochemistry, John Wiley and Sons, New York, 1966, p. 783.
[34] H. Nakanishi, H. Morita, S. Nagakura, Bull. Chem. Soc. Jpn. 50 (1977) 2255–2261.
[35] Y.S. Shon, G.B. Dawson, M. Porter, R.W. Murray, Langmuir 18 (2002) 3880–3885.
[36] F.D. Lewis, G.D. Salvi, D.R. Kanis, M.A. Ratner, Inorg. Chem. 32 (1993) 1251–1258.
[37] S. Giuffrida, G.G. Condorelli, L.L. Costanzo, I.L. Fragala, G. Ventimiglia, G. Vecchio, Chem. Mater. 16 (2004) 1260–1266.
[38] A.V. Veglia, R.H. De Rossi, J. Org. Chem. 58 (1993) 4941–4944.
[39] S. Sortino, S. Giuffrida, G. De Guidi, R. Chillemi, S. Petraia, G. Marconi, G. Condorelli, S. Sciuto, Photochem. Photobiol. 73 (2001) 6–13.
[40] O. Egyed, Vib. Spectrosc. 1 (1990) 225–227.
[41] N.V. Royk, L.A. Belyakova, J. Incl. Phenom. Macrocycl. Chem. 69 (2011) 315–319.
[42] J. Szejtly, Chem. Rev. 98 (1998) 1743–1753.
[43] K.B. Male, R.S. Brown, J.H.T. Luong, Enzyme Microb. Technol. 17 (1995) 607–614.
[44] J. Park, J. Joo, G.S. Kwon, Y. Jang, T. Hyeon, Angew. Chem. Int. Ed. 46 (2007) 4630–4660.
[45] M.B. Kasture, P. Patel, A.A. Prabhune, C.V. Ramana, A.A. Kulkarni, B.L.V. Prasad, J. Chem. Sci. 120 (2008) 515–520.
[46] A.V. Kabashin, M. Meunier, C. Kingston, J.H.T. Luong, J. Phys. Chem. B 107 (2003) 4527–4531.
[47] L.F. Liotta, Appl. Catal. B: Environ. 100 (2010) 403–412.
[48] M. Baldi, E. Finocchio, F. Milella, G. Busca, Appl. Catal. B: Environ. 16 (1998) 43–51.
[49] E.M. Cordi, P.J. O'Neill, J.L. Falconer, Appl. Catal. B: Environ. 14 (1997) 23–36.
[50] T.F. Garetto, C.R. Apesteguia, Catal. Today 62 (2000) 189–199.
[51] S. Minicò, S. Scirè, C. Crisafulli, R. Maggiore, S. Galvagno, Appl. Catal. B: Environ. 28 (2000) 245–251.
[52] T.F. Garetto, C.R. Apesteguia, Appl. Catal. B: Environ. 32 (2001) 83–94.
[53] N. Radic, B. Grbic, A. Terlecki-Baricevic, Appl. Catal. B: Environ. 50 (2004) 153–159.
[54] W.E. Kaden, W.A. Kunkel, M.D. Kane, F.S. Roberts, S.L. Anderson, J. Am. Chem. Soc. 132 (2010) 13097–13099.